A linear sampling method for inverse scattering elastodynamics problems in the time domain

S.H. Dehghan Manshadi & N. Khaji
Faculty of Civil and Environmental Engineering, Tarbiat Modares University, Tehran, Iran

SUMMARY:
This paper, deals with detecting and identifying unknown scatters (e.g., obstacles) in an elastic background solid through the use of elastic illuminating waves. In this regards, the Linear Sampling Method (LSM) for the reconstruction of the underground obstacles from near-field surface seismic measurements in the time domain is explained. The LSM is an effective approach to image the geometrical features of unknown targets. Although this method has been used in inverse acoustics problems dealing with far-field wave patterns in full space domains, there is no specific attempt to apply this method to the interpretation of near-field elastic wave forms in the time domain. It is found that the linear sampling method in the time domain working with a frequency band, improves the quality of the reconstruction of the obstacles compared to the frequency domain methods.

Keywords: Time domain linear sampling method, Qualitative inverse scattering, Elastodynamics.

1. INTRODUCTION

Inverse scattering problems deals with detecting and identifying, the reconstruction of unknown scatters (e.g., obstacles) in a background medium using measurement data of the scattered wave-fields, have been widely studied over the last few decades owing to their applications in a broad range of scientific and engineering disciplines such as seismology, non-destructive evaluation (NDE), medical diagnosis geophysics or submarine detection. We are interested in the non-destructive testing application where data such as the location and the nature of the obstacle are wanted, given a minimum number of observations. These inverse scattering problems have led to the development of the so-called qualitative methods for non-iterative obstacle reconstruction from far/near measurements of the scattered field. These methods provide a powerful alternative to the ordinary optimization approaches. These techniques can be classified as probe or sampling methods such as linear sampling method (LSM), topological sensitivity (TS), factorization method, the probe method, and point source method. The LSM is introduced in the inverse scattering literature by Colton and co-workers (1992, 1996). Although the LSM has gained remarkable attention in inverse scattering theory dealing with wave patterns in the frequency domain, little attention has been devoted to its application for near-field elastic wave forms in time domain. This is especially the case for the problems arising in the half-space domains during active seismic imaging of underground unknown scatters. As the aperture shrinks (e.g., the half space), the identification of the obstacle in time domain yields significantly better reconstructions by using continuum frequencies. The method aims at reconstructing the shape of an object from the knowledge of the multi time dependent-view data matrix U_s collected on the measurement domain Γ by means of N_r receiving and N_s transmitting probes. Such a goal is pursued by partitioning the investigated region Ω into an arbitrary grid of sampling points (z) and solving the linear matrix equation in each sampling point.

2. DIRECT SCATTERING PROBLEM

A two-dimensional scattering of elastic waves by a bounded buried cavity D with boundary ∂D as shown in Fig.2.1 is considered. With reference to a Cartesian coordinate system $\{\xi_1, \xi_2\}$, the half space $\{(\xi_1, \xi_2)|\xi_2 \geq 0\}$ is characterized by the Lame's constants λ and μ, mass density ρ. The material response is assumed to be linear elastodynamic.

The direct scattering problem investigates wave propagation in the exterior domain Ω and finding the scattered field $u_s(x, t)$ that satisfies the homogeneous Navier's equation (Achenbach, 1984)

$$(\lambda + \mu)\nabla(\nabla.U_s(\xi,t;\zeta)) + \mu\nabla^2 U_s(\xi,t;\zeta) = \rho\ddot{U}_s(\xi,t;\zeta), \qquad \xi \in \overline{\Omega}, \quad \zeta \in \Gamma, \tag{2.1}$$

and the boundary conditions

$$\begin{aligned}
u^{sk}(\xi,t;\zeta) &= u^{tk}(\xi,t;\zeta) - u^{ik}(\xi,t;\zeta), & \xi &\in \overline{\Omega}, & \zeta &\in \Gamma \\
\overline{\Omega} &= \Omega \setminus (D \cup \Gamma) \\
t^{tk}(\xi,t;\zeta) &= 0, & \xi &\in \Gamma, & \zeta &\in \Gamma, \\
t^{Sk}(\xi,t;\zeta) &= -t^{ik}(\xi,t;\zeta), & \xi &\in \partial D, & \zeta &\in \Gamma,
\end{aligned} \tag{2.2}$$

In the above equation, u^{tk} and u^{ik} are total displacement in the presence of scatterer and displacement in the absence of scatterer. t^{tk} indicates the traction vector whose value on the boundary of scatterer is zero, if the obstacle is cavity. The scattered field should also satisfy the Sommerfield radiation condition (Graff, 1991).

A two-dimensional spectral finite element model with absorbing boundary conditions has been developed to generate the synthetic data which is able to simulate wave scattering propagation in solid half-space. Combining excellent characteristics of classical finite element method (FEM) and spectral elements, spectral finite element method (SFEM) not only exhibits flexibility and ease of formulation, which is a FEM character, but also exploiting high order spectral elements leads to a significant superiority over FEM from the viewpoints of solution precision and computation costs (Komatitsch, 1998, 1999, 2000). Orthogonal basis functions are used as approximation functions and such selection of approximation functions in conjunction with specific numerical integrating schemes used in SFEM, leads to a diagonal mass matrix which is a great advantage over FEM. Fourier series, Chebyshev and Legendre polynomials are the commonly used basis functions. SFEM plays an important role in solving elastic wave propagation problems (Khaji et al, 2012)

The computer code based on SFEM, provides us the scattered displacement in time stepping Δt

$$u^s(\xi_i, n\Delta t; \zeta_j), \qquad i = 1,2,...,N_r, \quad n = 1,2,...,N_t, \quad j = 1,2,...,N_s \tag{2.3}$$

where ξ_i, ζ_j are receivers/point sources location, N_r and N_s are the number of receiver and source respectively. N_t is the number of time stepping and corresponds the final time recording.
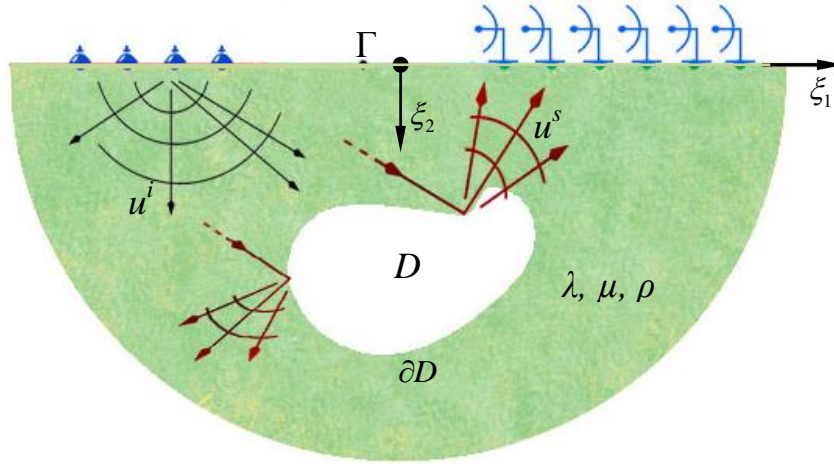
Figure 2.1. Excitation of an underground cavity in the half-space.

3. INVERSE SCATTERING PROBLEM

In this section we introduce the major notions and notations of the linear sampling method. It is assumed that a set of measurements of near field scattering pattern of incident point sources is available, each of these measurements corresponding to illumination of the medium. This problem is commonly referred in the literature as the 'inverse scattering' problem.

3.1. LINEAR SAMPLING METHOD

The LSM is an inverse scattering strategy to reconstruct the shape of an unknown scatterer from multi-view data collected from measurements of casual waves (Cakoni et al, 2006, 2011). This goal is pursued by partitioning the investigated region into an arbitrary grid of sampling points and by solving in each of them a linear equation. In particular, the idea of the method is to look for a superposition of the scattered fields (u_s) that, for each sampling point, matches with a prescribed radiating solution to the homogeneous Navier's equation in $\overline{\Omega}$ due to a point source acting at z in the direction of d. The statement of the method is that the L^2 norm of the solution to this problem is significantly larger outside the scattering object than inside. The mathematical formulation of the LSM relies on the layer potentials and operators. With respect to an arbitrary grid of points (z) that samples Ω, the LSM requires to solve in each sampling point the matrix equation (Nintcheu Fata, 2004)

$$N_d g_{z,\tau',d} = \phi_{z,\tau'} . d \qquad \|d\| = 1 \tag{3.1}$$

where $N_d g$ is the scattered field associated with the incident field and N_d is the near field operator. Time domain version of linear sampling method has a convolution structure and corresponds to the scattered fields (casual data)

$$
\begin{aligned}
(N_d g)(\xi, t) &= \iint_{R\,\Gamma_i} u_s(\xi, t; \zeta_0, t_0)\, g(\zeta_0, t_0)\, d(\zeta_0, t_0) \\
&= \iint_{R\,\Gamma_i} u_s(\xi, t - t_0; \zeta_0, 0)\, g(\zeta_0, t_0)\, d(\zeta_0, t_0)
\end{aligned}
\tag{3.2}
$$

Equation (3.2) can be formulated as near field operator equation of the form

$$(N_d g)(i,n) := \sum_{m=0}^{n} \sum_{j=1}^{N_x} u(x_i,(n-m)\Delta t; x_j, 0) g(j,m) \qquad N_d : R^{N_s \times N_t} \to R^{N_r \times N_t} \qquad (3.3)$$

In Eq. (3.1), $\phi_{z,\tau'}$ is the $N_t \times N_r$ dimensional vector contains the field radiated at the N_r receiving positions on by an elementary source located in $z \in \Omega$, and has a convolution structure (Duhamel integral)

$$\phi_{z,\tau'}(\xi,t) = \int_R G(\xi - z, t - \tau' - \tau) f(\tau) d\tau, \qquad \xi \in R^2 \setminus \{z\}, t \in R \qquad (3.4)$$

$f(\tau) \in C_c^\infty(R)$ is excitation force at sampling points and G denotes the fundamental solution for the wave equation (Chen et al, 2010). In the above equation, τ' corresponds to time shift and depends on the distance between the location of source and receiver. Therefore, the time shift for each sampling points can be changed. In fact, this parameter is related to the velocity of wave propagation in half-space elastic medium. With the best choice of τ', reconstruction of the obstacle can be improved.

The objective is to find the vector density $g_{z,\tau',d} \in L^2(\Gamma_1)$ as a solution to the near-field integral equation of the first kind whose $L^2(\Gamma_1)$-norm (i.e., the "energy") can be used as an indicator function for $\overline{\Omega}$ (Catapano et al, 2007). Since this norm is bounded inside D, it blows up on ∂D and can be made arbitrarily large outside D. In other words, the overall energy of these sampling points is an indicator of the obstacle, as it will achieve large values in sampling points external to the obstacle and lower values elsewhere (Aramini et al, 2010, 2011).

3.2. REGULARIZATION

In general, there is a fundamental difference between the forward and the inverse problems. Although the forward scattering problem is linear and well-posed, the inverse scattering problem is non-linear and ill-posed or improperly-posed in the sense of Hadamard. In his lectures, Hadamard believed that mathematical models of physical phenomena has to be well-posed if

1. A solution of the problem exists (existence).
2. The solution is unique (uniqueness).
3. The solution depends continuously on the data (stability).

Problems that are not well-posed in the sense of Hadamard are termed ill-posed. The LSM can be considered as a Fredholm integral equation of the first kind with an analytical kernel function, which is severely ill-posed or improperly-posed in the sense of Hadamard (Kirsch, 2011). The integral operators are compact. Hence, a small error in input data causes a large error in the shape reconstruction process which may lead to instability. Consequently, as an approximation to the integral operator, the interpolation matrix N_d is severely ill-conditioned. The accurate and stable solution of Equation (3.2) is very important for obtaining physically meaningful numerical results. Regularization methods are among the most popular and successful methods for solving stably and accurately ill-conditioned matrix equations. In our computations, we use the Tikhonov regularization to solve the matrix equation arising from the LSM discretization. Regularized solution of (3.1) can be found by minimizing the Tikhonov functional (Colton et al, 1997, 2000)

$$F_{Thikhonov}(g_{z,\tau',d}; \lambda) = \left\| N_d g_{z,\tau',d} - \phi_{z,\tau'} \right\|^2_{L^2(\Omega)} + \lambda \left\| g_{z,\tau',d} \right\|^2_{L^2(\Omega)} \qquad (3.5)$$

where $\lambda > 0$ is known as the Tikhonov regularization parameter. In our computations, we choose λ by the Morozov principle and is computed as

$$f(\lambda) = \sum_{i=1}^{M} \frac{\lambda^2 - \delta^2 \sigma_i^2}{(\sigma_i^2 + \lambda)^2} \left| \left(U^* \phi_{z,\tau'} \right) \right|^2$$

(3.6)

In equation (3.6), δ is the error of operator N_d which is computed using $\left\| N_d^\delta - N_d^{comp} \right\| \leq \delta$. To solve Equation (3.1), the singular value decomposition of N_d is computed as $N_d = U \, S \, V^*$, where U and V are $(N_t \, N_s) \times (N_t \, N_r)$ unitary matrices, V^* is the transpose of V, and S is a diagonal matrix with $S_{ii} = \sigma_i$. With reference to (3.5), the norm of a Tikhonov-regularized solution $g_{z,\tau',d}$ to (3.1), with regularization parameter λ is accordingly computed as

$$\left\| g_{z,\tau',d} \right\|_{L^2(\Omega)}^2 = \sum_{i=1}^{M} \frac{\sigma_i^2}{\left(\sigma_i^2 + \lambda \right)^2} \left| \left(U^* \phi_{z,\tau'} \right)_i \right|^2 \ .$$

(3.7)

With the plot of $1 / \left\| g_{z,\tau',d} \right\|$ as indicator function, the support of the unknown scatterer can be determined.

4. NUMERICAL EXAMPLES

This section is devoted to presenting numerical results demonstrating the capability of the time-domain linear sampling method to provide good reconstruction of an underground cavity in the half-space with data available on the free surface. The force is assumed to vary in time as a Ricker wavelet whose equation is

$$f(t) = a(1 - 2\tau^2) e^{-\tau^2} \ , \qquad \tau = (t - t_s)/t_0$$

(4.1)

where t_s is the time at which the maximum occurs, a is the amplitude, and corresponds to the dominant period of the wavelet. For this study, t_0 was set to 0.1 which corresponds to a dominant frequency of the wavelet near 14.5 Hz. The function $f(t)$ and its spectrum are depicted in Fig. 4.1.

(a)   (b)
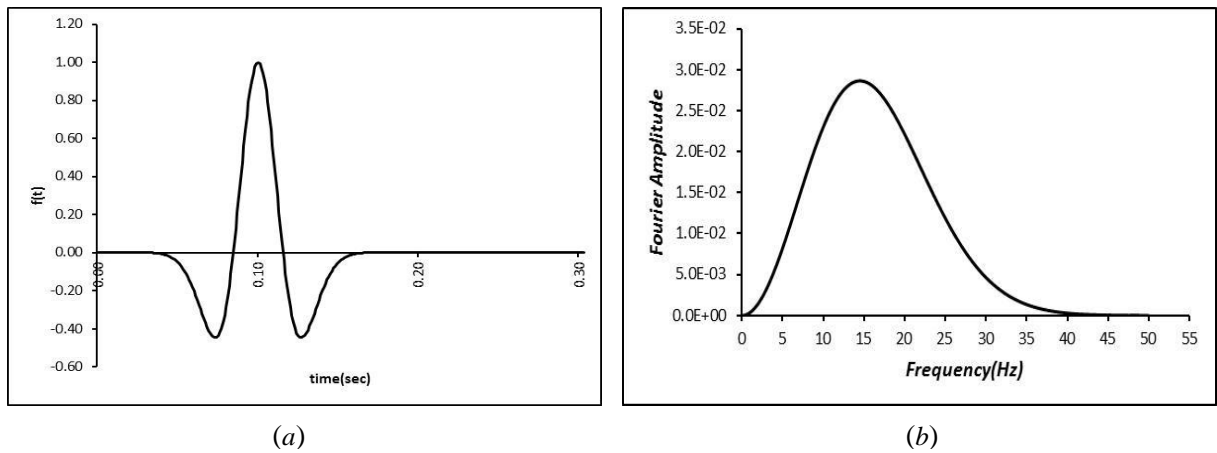
Figure 4.1. (a) Ricker wavelet, (b) The Fourier transform of the Ricker wavelet.

4.1. RECONSTRUCTION OF A SINGLE-CAVITY

The numerical example deals with the elastic-wave imaging of a rectangular void embedded in a half-space solid as depicted in Fig. 4.2. With reference to the Cartesian frame, {O; x, y}, the cavity is centred at (2000, 1000). The location of the sources and measurements location are on the free surface and compatible. The isotropic elastic half-space medium has a P-wave velocity of 3200 m/s, a S-wave velocity of 1847.5 m/s, a mass density of 2200 kg/m^3, and is modelled as a domain of size 4000 × 2000 m^2 in plane strain conditions. In the simulation, the cavity is exposed sequentially using 25 source points similar to Lamb problem. From each source point, the void is illuminated in sequence using Ricker forces acting in two perpendicular directions (x, y). In all subsequent simulation, the total time of response to be calculated is 2 sec and the time step used in this experiment is $\Delta t = 0.001$. For every point source in Lamb and Garvin problem, synthetic data is obtained using the spectral finite element method. For the forward numerical solution, we use a mesh of 50 × 25 elements, with a polynomial approximation of order N = 5. Fig. 4.3 (a), typically displays the total vertical displacement in the presence of cavity, in receiver located at (800, 2000) due to source point at (1760, 2000) in y-direction. Similarly, this process is done for perfect model (i.e., without cavity). When the differences of two signals are calculated, the influence of the cavity comes out, as shown in Fig. 4.3 (b). These differential waveforms as a forward solution will be used in the time version of linear sampling method to detect an existing cavity in the half-space medium.
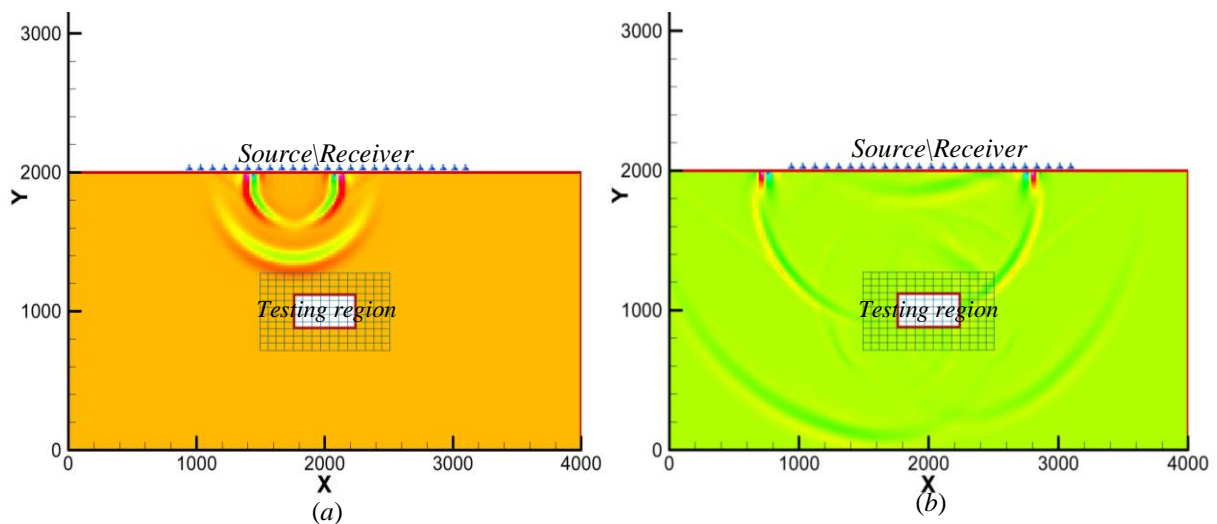
Figure 4.2. Reference geometry and investigated region of the half-space imaging problem and wave profiles at time (*a*) 0.3sec (*b*) 0.7sec in the Lamb's problem.
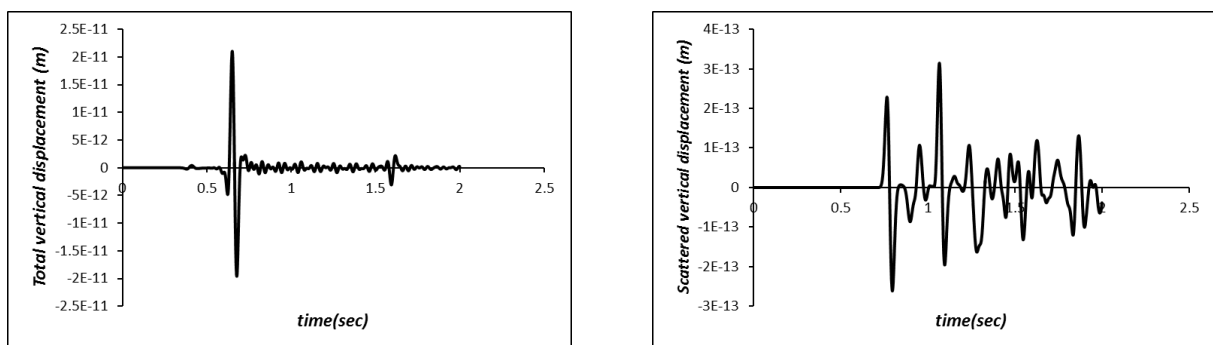
Figure 4.3. The time histories of vertical displacement in receiver located at (800, 2000) for (*a*) total and (*b*) scattered response.

In this numerical example, $M = 5000$ singular values for evaluating the Equation (3.6) are used. Figure 4.4 shows the decay of first 300 singular values of the discrete near-field operator N_d. The number of singular values which are used in time version of linear sampling method is more than frequency version of LSM. In fact, intensity variation of singular values in frequency domain is much more than time domain.

In our numerical example, we consider $\tau' = 0.20\sec$. The appropriate choice of time shift plays an important role in our reconstructions. With synthetic data calculated using spectral finite element, LSM equation is solved for the density $g_{z,\tau',d}$ at a 16×12 grid of sampling points, uniformly spaced over a 1200×800 rectangular testing region. In the simulation, a fictitious Ricker point source with polarization $d=(0,1)^T$, is determined at every sampling point z. Fig. 4.5 illustrates the variation of $1/\left\|g_{z,\tau',d}\right\|_{L^2(\Omega)}$ as a function of sampling point, time shift and source polarization obtained using (3.6) with λ= 9.53×10^{-7}. As one expects, the value of $1/\left\|g_{z,\tau',d}\right\|_{L^2(\Omega)}$ inside the cavity is large. The dashed line indicates the true boundary of rectangular cavity.
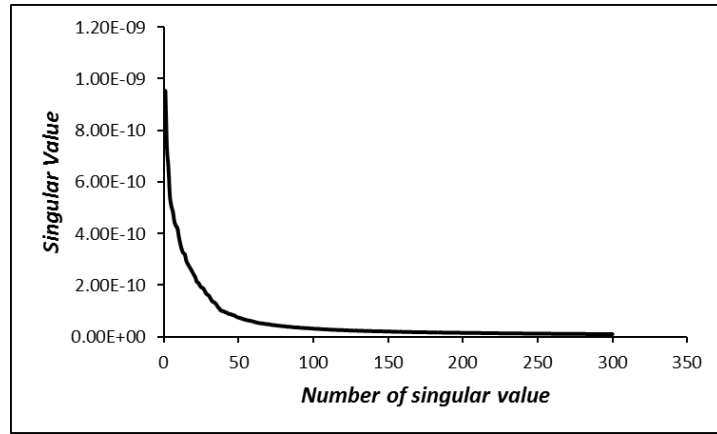
Figure 4.4. The decay of first 300 singular values of the discrete near-field operator N_d .
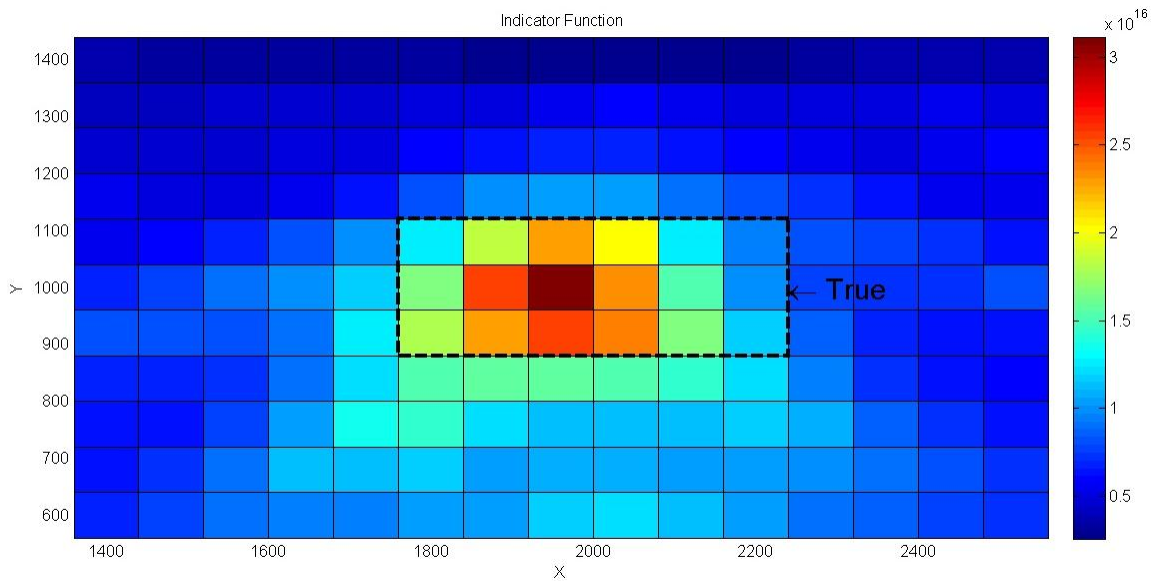
Figure 4.5. Contour plot of the indicator function $1/\left\|g_{z,\tau',d}\right\|_{L^2(\Omega)}$ for the identification of a rectangular cavity

using two axial point source.

5. CONCLUSIONS

In this study, the problem of reconstructing two-dimensional cavity embedded in a half-space solid from near-field, surface seismic observations is investigated by means of the linear sampling method in time domain that is rooted in far-field acoustics and electromagnetic. We have shown that it is possible to exploit the LSM in the framework of time domain to obtain a qualitative reconstruction of unknown scatterers with a limited number of receivers/transmitters on the free surface of half-space domain. In this case, the time domain version of linear sampling method provides satisfactory reconstructions of the obstacles due to working with a frequency band.

REFERENCES

Colton, D., and Kress, R. (1992). Inverse Acoustic and Electromagnetic Scattering Theory (Berlin: Springer)

Colton, D. and Kirsch, A. (1996). A simple method for solving inverse scattering problems in the resonance region. Inverse Problems **12,** 383–93.

Achenbach, J. D. (1984). Wave Propagation in Elastic Solids. Amsterdam: North-Holland.

Graff, K. F. (1991). Wave Motion in Elastic Solids. New York: Dover.

Komatitsch, D., Vilotte, J.P. (1998). The spectral element method: An efficient tool to simulate the seismic response of 2D and 3D geological structures. B Seismol Soc Am **88:**368–92.

Komatitsch, D., Vilotte, J.P., Vai, R., Castillo-Covarrubias, J.M. and Sanchez-Sesma, F.J. (1999). The spectral element method for elastic wave equations-application to 2-D and 3D seismic problems. Int J Numer Meth Eng;**45:**1139–1164.

Komatitsch, D., Barnes, C., Tromp, J. (2000). Simulation of anisotropic wave propagation based upon a spectral element method. Geophysics;**65:**1251–1260.

Khaji, N., Kazemi Noureini, H. (2012). Detection of a Through-Thickness Crack Based on Elastic Wave Scattering in Plates, Part I: Forward Solution, Asian Journal of Civil Engineering, **13(3)**, 301–318.

Kazemi Noureini, H., Khaji, N. (2012). Detection of a through-thickness crack based on elastic wave scattering in plates, Part II: Inverse Solution, Asian Journal of Civil Engineering, **13(4)**, 433–454.

Cakoni, F. and Colton, D. (2006). Qualitative Methods in Inverse Scattering Theory. Springer-Verlag, Berlin, Heidelberg, Germany.

Cakoni, F., Colton, D., Monk, P. (2011). The linear sampling method in inverse electromagnetic scattering. SIAM-Society for Industrial and Applied Mathematics.

Nintcheu Fata, S. and Guzina, B. B. (2004). A linear sampling method for near-field inverse problems in elastodynamics. Inverse Problems **20.** 713–736.

Chen, Q., Haddar, H., Lechleiter, A. and Monk, P. (2010). A sampling method for inverse scattering in the time domain. Inverse Problems **26, 085001**.

Catapano, I., Crocco, L., and Isernia, T. (2007). On simple methods for shape reconstruction of unknown scatterers. IEEE Trans. Antennas Propag., **55:5,**1431–1436.

Aramini, R., Caviglia, G., Massa, A., and Piana, M. (2010). The linear sampling method and energy conservation. Inverse Problems **26**, p. 055004.

Aramini, R., Brignone, M., Caviglia, G. Massa, A. and Piana, M. (2011). The linear sampling method in a lossy background: an energy perspective, Inverse Problems in Science and Engineering, 1–22.

Kirsch, A. (2011). An Introduction to the Mathematical Theory of Inverse Problems. Springer-Verlag, Berlin, Heidelberg, Germany.

Colton, D., Piana, M. and Potthast, R. (1997). A simple method using Morozov's discrepancy principle for solving inverse scattering problems. Inverse Problems **13,** 1477–93.

Colton, D., Coyle, J. and Monk, P. (2000). Recent developments in inverse acoustic scattering theory. SIAM Rev. **42,** 369–414.